Bioinformatics Advance Access published March 7, 2007

BIOINFORMATICS

# From Structure to Dynamics of Metabolic Pathways: Application to the Plant Mitochondrial TCA Cycle

Ralf Steuer [a,c], Adriano Nunes Nesi [b], Alisdair R. Fernie [b], Thilo Gross [c], Bernd Blasius [c], and Joachim Selbig [a,b]

[a]University Potsdam, Institute for Biochemistry and Biology, Karl-Liebknecht-Strasse 24-25, Haus 20, 14476 Potsdam, Germany. [b]Max-Planck-Institute of Molecular Plant Physiology, Am Mühlenberg 1, 14476 Potsdam, Germany. [c]University Potsdam, Institute for Physics, Nonlinear Dynamics Group, Am Neuen Palais 10, 14469 Potsdam, Germany.

Associate Editor: Prof. Alfonso Valencia

## ABSTRACT

**Motivation:** Mitochondrial metabolism, dominated by the reactions of the tricarboxylic acid (TCA) cycle, is of vital importance for a wide range of metabolic processes. In particular for autotrophic tissue, such as plant leaves, the TCA cycle marks the point of divergence of anabolic pathways and plays an essential role in biosynthesis. However, despite extensive knowledge about its stoichiometric properties, the function and the dynamical capabilities of the TCA cycle remain largely unknown.

**Methods and Results:** Based on a recently proposed formalism, we investigate the dynamic and functional properties of the mitochondrial TCA cycle of plants. Starting with the structural properties, as described by the elementary flux modes of the system, we aim for the transition from structure to the dynamics of the TCA cycle. Using a parametric description of the system, encompassing all possible differential equations and parameter values, we detect and quantify regimes of different dynamic behavior. Optimizing the system with respect to dynamic stability, we demonstrate that maximal stability is associated with specific (relative) metabolite concentrations and flux values that are subsequently compared to the experimental literature. Our analysis also serves as a general example how to elucidate the transition from the structure to the dynamics of metabolic pathways.

**Contact:** steuer@agnld.uni-potsdam.de

## INTRODUCTION

Over the last decade, significant advances in experimental high-throughput techniques have resulted in unprecedented information about the components that constitute cellular metabolism (Fernie *et al.*, 2004; Sweetlove & Fernie, 2005). In particular, the genome-scale reconstruction of metabolic networks has revolutionized the ability to understand and engineer metabolic function, along with the possibility to predict metabolic phenotypes and key aspects of network functionality (Schuster *et al.*, 1999, 2000; Stelling *et al.*, 2002; Famili *et al.*, 2003).

However, the stoichiometric properties alone are not sufficient to define and predict the dynamical behavior of complex cellular systems (Ronen *et al.*, 2002; Ingram *et al.*, 2006). One of the primary challenges for post-genomic computational biology thus remains to bridge the gap between network structure on the one hand, and the resulting dynamic properties of metabolic systems on the other hand. Usually, the latter is accomplished by translating metabolic processes into a set of differential equations, requiring extensive additional (and often unavailable) information about the kinetic parameters and the specific functional form of the rate equations.

Recently, we have proposed an alternative formalism that allows to quantitatively evaluate the possible dynamics of metabolic systems without referring to any explicit set of differential equations (Steuer *et al.*, 2006). Our approach is based upon a parametric representation of the Jacobian matrix of a metabolic system, such that each element of the Jacobian has a well-defined and straightforward interpretation in biochemical terms. Instead of focusing on a particular set of differential equations, this parametric representation allows to evaluate large ensembles of possible models, each restricted to comply with the available biochemical knowledge. In this way, it is possible to evaluate the stability with respect to perturbations, the existence of bifurcations and oscillatory regions, as well as several other characteristic dynamic features of the system.

Utilizing this approach, we aim to investigate the robustness and possible dynamics of the mitochondrial TCA cycle of plant leaves. In the first section, we outline the structural and stoichiometric properties of the system, making use of the concept of elementary flux modes (Schuster *et al.*, 1999). Subsequently, after a brief synopsis of the mathematical background, we construct the parametric representation of the Jacobian matrix of the plant mitochondrial TCA cycle. In the following sections, we characterize the stability of the system with respect to perturbations and evaluate the existence and size of oscillatory regions. It is demonstrated that our method allows to identify specific biochemical conditions that result in an increased stability of the system. In the last section, we discuss our results and point out a general strategy to elucidate the transition from structure to dynamics of biochemical pathways.

## A MODEL OF THE TCA CYCLE

In plants the role of the TCA cycle differs fundamentally from that in heterotrophic organisms. Due to their autotrophic nature, plants synthesize their own respiratory substrates, mainly carbohydrates, which then serve as the main substrates for the TCA cycle. In addition to the synthesis of ATP, the TCA cycle marks a point of divergence of anabolic pathways and provides precursors for a number of biosynthetic processes, such as nitrogen fixation and the biosynthesis of amino acids (Hill, 1997).

Figure 1 depicts a simplified representation of the TCA cycle, which will be investigated in the following sections. As the main substrate,

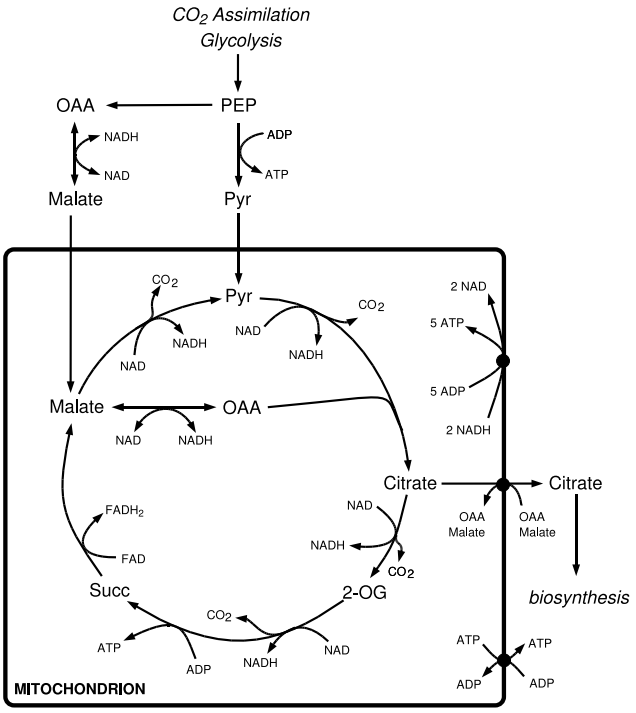


**Fig. 1.** A schematic representation of the TCA cycle for plant leaf tissue. A detailed list of reactions is given in Table 1. For simplicity, several metabolic intermediates are omitted from the cycle and export of main metabolic intermediates is restricted to citrate, in strict exchange for either OAA or malate. For abbreviations see Table 1.

**Table 1.** Main reactions of a model of the TCA cycle. The system consists of 16 reactions, including simplified overall reactions. ATP is synthesized from NADH and subsequently exported to the cytosol. Export of metabolic intermediates is restricted to citrate. The contribution of $FADH_2$ to energy production is neglected. Abbreviations are: PEP (phosphoenolpyruvate), Pyr (pyruvate), OAA (oxaloacetate), Mal (Mal), Cit (citrate), 2-OG (2-oxoglutarate), Succ (succinate). The subscript *cyt* denotes cytosolic metabolites.

| number | | reaction |
|---|---|---|
| | | **Cytosol** |
| 1 | $\nu_{1c}$ | Glycolysis $\rightarrow$ $PEP_{cyt}$ |
| 2 | $\nu_{2c}$ | $PEP_{cyt}$ + $ADP_{cyt}$ $\rightarrow$ $ATP_{cyt}$ + $Pyr_{cyt}$ |
| 3 | $\nu_{3c}$ | $PEP_{cyt}$ $\rightarrow$ $OAA_{cyt}$ |
| 4 | $\nu_{4c}$ | $OAA_{cyt}$ + $NADH_{cyt}$ = $NAD_{cyt}$ + $Mal_{cyt}$ |
| | | **Transport** |
| 5 | $\nu_{1T}$ | $Pyr_{cyt}$ $\rightarrow$ Pyr |
| 6 | $\nu_{2T}$ | $Mal_{cyt}$ $\rightarrow$ Mal |
| 7 | $\nu_{3Ta}$ | Cit + $OAA_{cyt}$ $\rightarrow$ OAA + $Cit_{cyt}$ |
| 8 | $\nu_{3Tb}$ | Cit + $Mal_{cyt}$ $\rightarrow$ Mal + $Cit_{cyt}$ |
| | | **Mitochondrion** |
| 9 | $\nu_1$ | Pyr + NAD + OAA $\rightarrow$ Cit + NADH + $CO_2$ |
| 10 | $\nu_2$ | Cit + NAD $\rightarrow$ NADH + 2-OG + $CO_2$ |
| 11 | $\nu_3$ | 2-OG + NAD + ADP $\rightarrow$ Succ + NADH + ATP + $CO_2$ |
| 12 | $\nu_4$ | Succ +FAD $\rightarrow$ $FADH_2$ + Mal |
| 13 | $\nu_5$ | Mal + NAD = OAA + NADH |
| 14 | $\nu_6$ | Mal + NAD $\rightarrow$ Pyr + NADH + $CO_2$ |
| | | **Energy** |
| 15 | $\nu_{1E}$ | 2 NADH + 3 ADP $\rightarrow$ 2 NAD + 3 ATP |
| 16 | $\nu_{2E}$ | ATP + $ADP_{cyt}$ $\rightarrow$ ADP + $ATP_{cyt}$ |

we consider phosphoenolpyruvate (PEP), metabolized via glycolysis and the oxidative pentose phosphate pathway. PEP is then either converted to pyruvate (Pyr) or to oxaloacetate (OAA), with a subsequent conversion to malate (Mal). Pyruvate and malate enter the mitochondrion. In Fig. 1, the export of metabolic intermediates for biosynthesis is restricted to citrate (Cit), in strict exchange of either OAA or malate. Note that the TCA cycle in plants lacks the glyoxylate shunt. With pyruvate as the only substrate, the TCA cycle is not able to catalyze a net synthesis of its metabolic intermediates (Hill, 1997).

### Structural Analysis: Elementary Flux Modes

Starting point of our analysis are the structural properties of the system, as described by the set of elementary flux modes depicted in Fig. 2. An elementary flux mode (EFM) is defined as a minimal set of reactions that is consistent with a valid steady state, i.e. it defines a flux distribution that fulfills the stoichiometric mass-balance equation (Heinrich & Schuster, 1996; Schuster *et al.*, 1999). The term 'elementary' refers to the nondecomposability of modes, i.e. an EFM cannot be represented by a combination of two or more smaller elementary fluxmodes (Schuster *et al.*, 1999, 2000).

The TCA cycle, as depicted in Fig. 1, gives rise to 6 elementary fluxmodes, corresponding to different modes of operation: **EFM A:** Pyruvate is imported into the mitochondrion. No metabolic intermediates are exported. Note that in this situation the cycle is subject to a mass-conservation relationship, i.e. the total amount of malate, OAA, citrate, 2-OG and succinate is preserved. The cycle is thus not able to catalyze a net synthesis of its intermediates. However, in the presence of the NAD-malic enzyme (reaction $\nu_6$ in Table 1), converting malate to pyruvate, this inevitably results in a depletion of metabolic intermediates and already indicates a potential dynamic instability of the pathway. **EFM B:** Malate substitutes for pyruvate as substrate for the TCA cycle. In this case, pyruvate and OAA are both synthesized from malate. **EFM C:** As an alternative mode of operation, the TCA cycle provides citrate as a precursor for biosynthesis. The total amount of citrate and OAA within the mitochondrion is preserved. **EFM D:** Same as EFM C, only malate substitutes for OAA uptake in exchange with citrate. Note that in this case, the presence of the NAD-malic enzyme again results in a depletion of metabolic intermediates. **EFM E and F:** Same C and D, but with malate substituting for pyruvate import.

## A STRUCTURAL KINETIC MODEL

Given knowledge about the structural and stoichiometric properties of the TCA cycle, we now aim for the transition from structure to dynamics of the system. In particular, a steady state flux distribution $\boldsymbol{\nu^0} = \boldsymbol{\nu}(\boldsymbol{S^0})$ that is consistent with the stoichiometric balance equation $\mathbf{N}\boldsymbol{\nu^0} = \mathbf{0}$ does not guarantee actual dynamic stability of the system. Taking dynamical properties of the system into account, we thus seek to elucidate the stability, robustness and possible dynamics of the pathway – based only on a minimal amount of additional information.

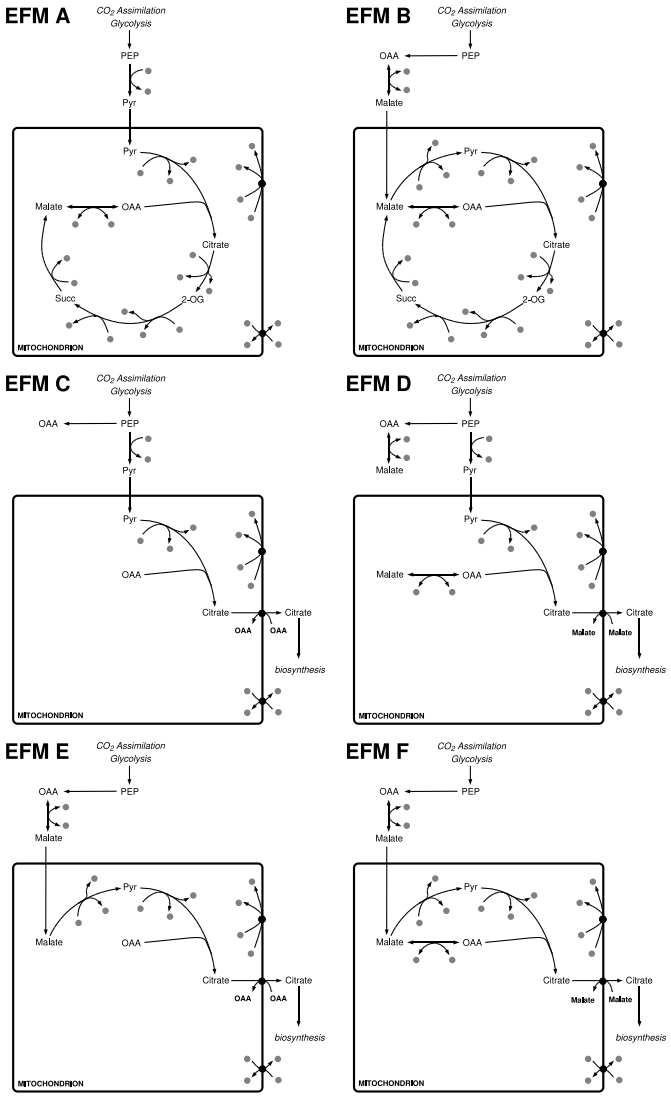


**Fig. 2.** The elementary flux modes of the TCA cycle depicted in Fig. 1. The system gives rise to 6 elementary modes A-F. For a description and details see text.

To this end, we have recently proposed a method that allows to asses the dynamic capabilities of a metabolic system without referring to any explicit set of differential equations (Steuer *et al.*, 2006). Our approach is based on a decomposition of the Jacobian $\mathbf{J}$ of a metabolic system, consisting of $m$ metabolites and $r$ reactions, into a product of two matrices, such that the elements of each matrix have a well-defined and straightforward interpretation in biochemical terms.

$$\mathbf{J_x} = \mathbf{\Lambda}\boldsymbol{\theta}^{\boldsymbol{\mu}}_{\boldsymbol{x}} \tag{1}$$

For a derivation of Eq. (1), as well as a simple example, see the Appendix. Within our parametric representation of the Jacobian, the $m \times r$ dimensional matrix $\mathbf{\Lambda}$ defines the time-constants of the system. Given knowledge of the stoichiometric matrix $\mathbf{N}$, a set of steady state metabolite concentrations $\mathbf{S^0}$, and a steady state flux distribution $\boldsymbol{\nu}^{\mathbf{0}}$, the matrix $\mathbf{\Lambda}$ is fully defined. The second term in Eq. (1) defines the saturation or *'effective kinetic order'* of each reaction with respect to the metabolites. For each element $\theta^{\mu}_{x}$ of the $r \times m$ dimensional matrix $\boldsymbol{\theta}^{\boldsymbol{\mu}}_{\boldsymbol{x}}$, we can specify a well-defined interval that covers all possible values of $\theta^{\mu}_{x}$, without referring to the explicit functional form of the rate equations.

Given the parametric decomposition of the Jacobian defined in Eq. (1), the non-zero elements of both matrices span the associated *parameter space* and uniquely define the Jacobian at each possible point in parameter space. We emphasize that this generalized parameter space is equivalent to the more usual description in terms of Michaelis constants and maximal reaction velocities A subsequent statistical evaluation of the Jacobian matrix then allows to assess several key dynamical properties of the system, such as the stability of steady states, relevant timescales (modal analysis), as well as the existence and location of possible bifurcations (Heinrich & Schuster, 1996; Steuer *et al.*, 2006).

## Application to the TCA Cycle Model

We now seek to apply our concept of structural modeling to the TCA cycle depicted in Fig. 1. Starting with the simplest possible model, we first neglect the contribution of cofactors and consider only the main metabolic intermediates. The corresponding dynamical system consists of $m = 9$ variables and $r = 13$ reactions. To specify the Jacobian, we need *i)* a set of steady state metabolite concentrations $\boldsymbol{S}^{\mathbf{0}}$; *ii)* a steady state flux distribution $\boldsymbol{\nu}^{\mathbf{0}}$, determined by $r - \mathrm{rank}(\mathbf{N}) = 4$ free parameters; and *iii)* a set of 14 saturation parameters $\theta^{\mu}_{x} \in [0, 1]$ specifying the degree of saturation of each reaction with respect to each of its substrates.

As a first approximation, all saturation parameters are set to unity $\theta^{\mu}_{x} = 1$, corresponding to a simple mass-action model of the system. Evaluating the resulting Jacobian for a large ensemble of randomly chosen flux and concentration values reveals that in this case the Jacobian is always rank deficient, i.e. the system does not allow for the existence of a dynamically stable steady state. Investigating this more closely, and testing for additional saturation parameters, reveals that the instability is resolved when the malate dehydrogenase $\nu_5$ is inhibited by its product OAA. Alternatively, the NAD-malic reaction $\nu_6$ needs to be inhibited by its product Pyr. Indeed, as could be expected intuitively, the instability results from a possible imbalance between the rate of Pyr and OAA production within the mitochondrion. Since the malate dehydrogenase is reversible, the instability is prevented in the actual biological system: Excess of OAA induces an increased flux from malate towards pyruvate. To account for this in the model, and to avoid the rank deficiency of the Jacobian, the parameters $\theta^{5}_{\mathrm{OAA}} = -0.1$ and $\theta^{6}_{\mathrm{Pyr}} = -0.1$ are fixed to weak inhibition in the following.

Resuming the analysis for the modified ensemble of Jacobians, the next question relates to the dynamic stability of the TCA cycle. Following the approach described in (Steuer *et al.*, 2006), we generate a large ensemble of possible models (Jacobians) by choosing the flux and concentration values from a random distribution. Subsequently, we select for those models that are maximally stable, i.e. those model that have a minimal largest real part $\lambda_R^{\max}$ within their spectrum of eigenvalues – corresponding to a fast response to perturbations. Within this constraint ensemble of maximally stable models, deviations in the distributions of individual parameters from their initial distribution indicate a relationship between these parameters and the stability of the model. Figure 3 compares the initial random distribution of all possible OAA concentrations to

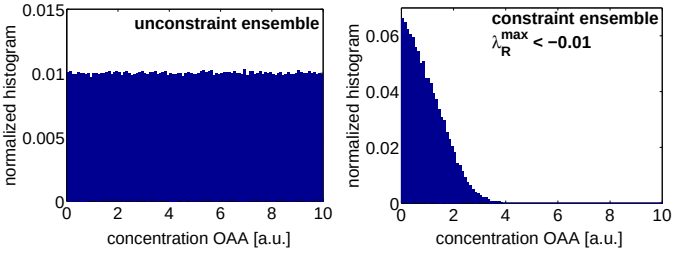


**Fig. 3.** Evaluating an ensemble of $10^6$ Jacobians with parameters drawn from a random distribution. *Left plot:* The initial distribution of steady state OAA concentration for the unconstraint ensemble. *Right plot:* The distribution of steady state OAA concentration for the constraint ensemble of Jacobians with a largest real part $\lambda_R^{\max} < -0.01$ within the spectrum of eigenvalues (corresponding to the $\sim 4\%$ of maximally stable models). Similar results are obtained for pyruvate. As the absolute values of concentrations are not relevant, all concentrations are measured relative to cytosolic Pyr and are chosen equally distributed in $S_i^0 \in [0, 10]$. Steady state flux values are chosen as random superpositions of fluxmodes, such that the total influx $\nu_{1c}^0 = 1$ equals unity. All saturation parameters are $\theta_x^\mu = 1$, except $\theta_{\mathrm{OAA}}^5 = -0.1$ and $\theta_{\mathrm{Pyr}}^6 = -0.1$.

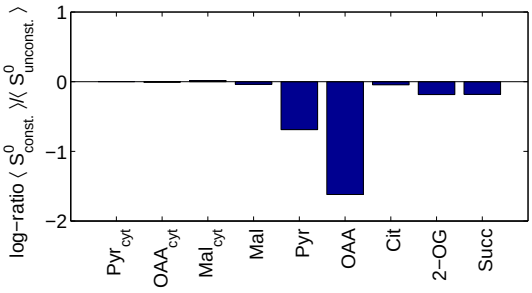


**Fig. 4.** Comparing the average steady state concentration of metabolites within the constraint ensemble of maximally stable models to the initial value. Shown is the ratio $\log[\langle S^0_{\mathrm{constraint}}\rangle / \langle S^0_{\mathrm{unconstraint}}\rangle]$. The largest deviation is found for OAA and Pyr, indicating that these metabolites have the largest impact on the stability of the model. All concentrations are measured relative to $\mathrm{Pyr}_{\mathrm{cyt}}$.

the distribution found within the maximally stable ensemble. As can be observed, models with maximal stability are associated with low concentrations of OAA. Similar results are obtained for pyruvate, while all other concentration parameters show no, or only little, deviation in their distribution. The results for the remaining metabolites are summarized in Fig. 4. Verifying this finding, we evaluate the distribution of the largest real part $\lambda_R^{\max}$ within the spectrum of eigenvalues, while fixing the steady state concentrations of OAA and Pyr to low values. This results in a marked shift of $\lambda_R^{\max}$ towards negative values, as compared to the initial distribution for the unconstraint ensemble. See Fig. 5 for a visualization. We thus can conclude that a low concentrations of OAA and Pyr contribute significantly to an increased stability of the system, i.e. the return to the steady state after a perturbation is accelerated for lower concentrations of OAA and Pyr. Indeed, a previous study of plant mitochondria supports the assumption of a low OAA concentration *in vivo* (MacDougall & ap Rees, 1991). Though the

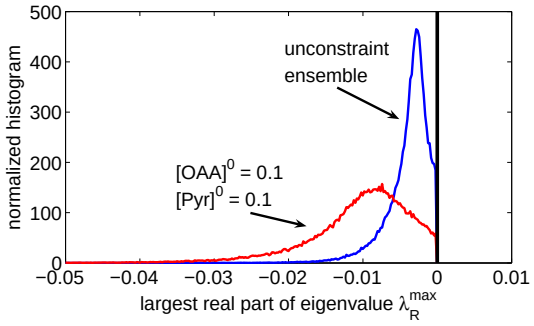


**Fig. 5.** Comparing the distribution of the largest real part $\lambda_R^{\max}$ within the spectrum of eigenvalues. For an ensemble of models (Jacobians) with low steady state concentrations of OAA and Pyr the distribution of $\lambda_R^{\max}$ is markedly shifted towards more negative values (red line), as compared to the unconstraint ensemble (blue line).

concentration could not be detected directly, an equilibrium assumption of the citrate synthase would result in $[\mathrm{OAA}]^0 \approx 10^{-8}$M, or about one molecule of OAA per mitochondrion (MacDougall & ap Rees, 1991). Thus, even when assuming that the citrate synthase is appreciably displaced from equilibrium, these results still indicates a rather low *in vivo* concentration.

Extending to analysis to the distribution of metabolic fluxes, we now evaluate the elementary flux modes, depicted Fig. 2, with respect to the dynamic stability of the system. When selecting for the maximally stable models among the ensemble of all possible models, most flux distributions attain a value close to the elementary modes EFM B and EFM F. Figure 6 shows a comparison of the contribution of the individual fluxmodes, with respect to the unconstraint ensemble. Note that the fluxmodes B and F rely on malate import only. This indicates that flux distributions relying on malate import, rather than pyruvate import, are favored with respect to their dynamic stability. Indeed, previous evidence shows that the capacity of the pyruvate transporter is rather low, and may be insufficient under some circumstances (Hill, 1997). Furthermore, transgenic tobacco plants, lacking any detectable cytosolic pyruvate kinase, were found to be indistinguishable from the wild-type (Hill, 1997).

## Bifurcations and Oscillations

In addition to the stability of the steady states, the parameterized Jacobian of the TCA cycle allows to infer a variety of other dynamic properties of the system. In particular, not all models (Jacobians) of the unconstraint ensemble are dynamically stable. A small fraction of about $3 \cdot 10^{-3}\%$ of the random realizations exhibit a pair of eigenvalues with positive real parts and conjugate imaginary parts. Exploring the parameter space in the vicinity of these realizations reveals the existence of a Hopf bifurcation. Figure 7 depicts a corresponding bifurcation diagram.

A Hopf bifurcation is usually associated with (at least transient) oscillatory behavior, as a pair of conjugate complex eigenvalues cross the imaginary axis. This is verified in Fig. 7 using an explicit model of the TCA cycle based on differential equations (see Appendix). However, we emphasize that the existence of oscillatory dynamics can be deduced from our parametric representation of the Jacobian alone, without referring to any explicit kinetic model of the system. Furthermore, we note that the oscillations arise solely due

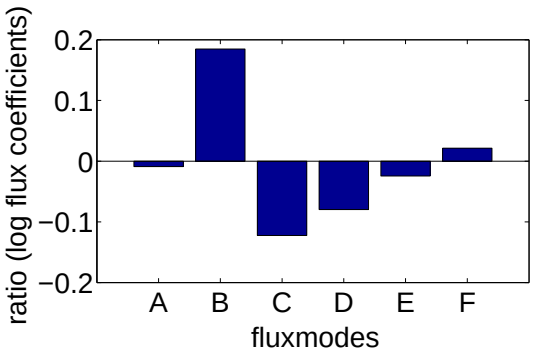


**Fig. 6.** Comparing the contribution of EFMs within the ensemble of most stable models. In the initial distribution, flux values are chosen randomly with $\boldsymbol{\nu^0} = \sum \alpha_i \, \mathbf{efm}_i$, such that the total input flux equals unity. Shown is the ratio $\log[\langle \alpha_i^{\text{constraint}} \rangle / \langle \alpha_i^{\text{unconstraint}} \rangle]$ for each EFM. Within the ensemble of most stable models, the EFMs B and F are overrepresented.

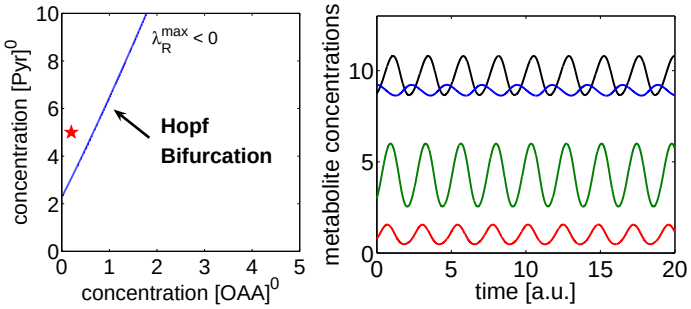


**Fig. 7.** *Left Plot:* A bifurcation diagram of the TCA cycle as a function of two parameters. At the Hopf bifurcation (blue line) the steady state looses its stability and (at least transient) oscillatory behavior must be expected. *Right Plot:* A numerical simulation of an explicit model of the TCA cycle, corresponding to a parameter set beyond the Hopf bifurcation (denoted with a red star on the left). Shown are the concentrations of malate (black line), 2-OG (blue line), pyruvate (green line), and cytosolic OAA (red line). Note that cytosolic OAA and malate oscillate due to the export of citrate. For details on the explicit model see Appendix.

to the stoichiometry of the system. As yet, all saturation parameters are set to unity and no allosteric interactions are included. Still, our analysis reveals the existence of an oscillatory region, confined to a small, but quantifiable, region in parameter space.

It should be noted that an analogous analysis of an explicit kinetic model, given in terms of the kinetic parameters of the reaction rates, is not trivial. Even when restricted to straightforward mass-action kinetics, involving only bilinear reaction terms, the steady state cannot be determined analytically. To evaluate possible bifurcations thus requires explicit numerical integration or other computationally costly methods. In contrast to this, our approach allows to directly specify the Jacobian of any desired steady state solution without any further computational assistance.

## EXTENDING THE MODEL

As yet, the analysis was restricted to non-saturable reaction rates with saturation parameters $\theta_x^\mu = 1$. Extending the model, we now

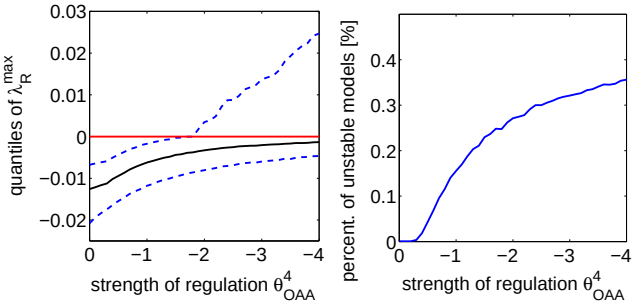


**Fig. 8.** Stability properties of the system as a function of the inhibition strength $\theta^4_{\text{OAA}}$ of OAA on the succinate dehydrogenase. For each value of $\theta^4_{\text{OAA}}$ an ensemble of Jacobians is generated and the distribution of the largest real parts $\lambda_R^{\max}$ is recorded. *Left Plot:* Shown is the median (solid black line), along with the $0.25$ and $0.75$ quantiles of the distribution of $\lambda_R^{\max}$ (with $\lambda_R^{\max} > 0$ corresponding to instability). *Right Plot:* The percentage of dynamically instable models ($\lambda_R^{\max} > 0$) as a function of $\theta^4_{\text{OAA}}$.

focus on a slightly different scenario, aiming to incorporate additional biochemical knowledge. In particular, we can make use of the fact that the *in vivo* flux distribution and the concentrations of many metabolic intermediates are known (see Appendix). Thus, instead of evaluating the Jacobian for all possible steady state concentrations and flux values, we restrict the model to comply with a specific experimentally observed steady state. Within the parametric representation of the Jacobian, this can be straightforwardly achieved by setting the matrix $\boldsymbol{\Lambda}$ constant.

In the following, by generating an ensemble of possible models (Jacobians) of the system at an observed steady state, we thus test for the stability and robustness of this specific state. All saturation parameters are allowed to take arbitrary values within their predefined interval, i.e., $\theta_S^\nu \in [0, 1]$ for any substrate of a reaction. The overall results agree qualitatively with the previous section: The vast majority of instances is dynamically stable, i.e. independent of the saturation (or non-saturation) of particular reactions, the observed operating point and flux values correspond to a stable steady state of the system – indicating a high robustness of the system with respect to the saturation of specific reactions. Only for a minor fraction of possible saturation parameters ($\sim 0.03\%$), the observed state is dynamically unstable. Again, we can select for the subset of maximally stable models and identify specific saturation parameters that contribute to an increased stability of the system (data not shown).

However, a more interesting situation arises if additional regulation is included into the model. In particular, OAA is known to inhibit the succinate dehydrogenase (included within $\nu_4$ in Table 1). Within the structural kinetic model, this gives rise to an additional saturation parameter $\theta^4_{\text{OAA}} \in [0, -n]$, where $n$ denotes a positive (integer) coefficient, specifying the maximal strength of the regulatory interaction. Figure 8 depicts the stability properties of the system at the observed state as a function of $\theta^4_{\text{OAA}} \in [0, -n]$: For an increasing strength of the regulation, the size of the region in parameter space that is associated with dynamic instability rapidly increases. In such a situation, the system cannot be considered robust with respect to the saturation of the reactions. Instead, our analysis then allows to uncover specific conditions and requirements for the experimentally observed state to be stable, i.e. to be actually observable

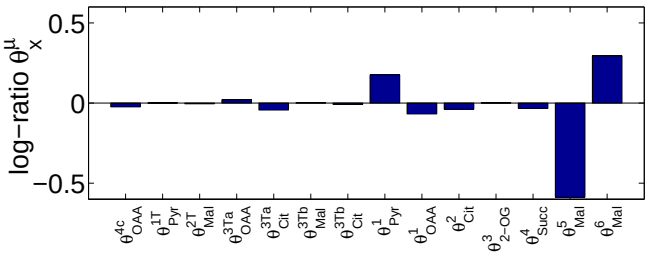


**Fig. 9.** Comparing average saturation parameters $\theta_x^S$ within the subset of unstable models to the unconstraint ensemble (for $\theta^4_{\mathrm{OAA}} = -4$). Strong saturation of $\nu_5$ (malate dehydrogenase) and low saturation of $\nu_6$ (NAD-malic reaction) favors instability. Vice versa, when setting $\theta^5_{\mathrm{Mal}} = 1.0$ (linear regime) and $\theta^5_{\mathrm{Mal}} = 0.1$ (strong saturation) the probability of finding $\lambda_R^{\max} > 0$ decreases ($0\%$ within $5 \cdot 10^4$ instances, compared to $\sim 35\%$ in the unconstraint ensemble.).

as a steady state of the system. Similar to the previous sections, we thus again compare the average saturation parameters $\theta_x^S$ within the subset of unstable models to the unconstraint ensemble. The result are summarized in Fig. 9 for all saturation parameters. As can be observed, strong saturation of the malate dehydrogenase (reaction $\nu_5$) and low saturation of the NAD-malic reaction (reaction $\nu_6$), both with respect to the substrate malate, favors instability.

## SUMMARY AND CONCLUSIONS

The TCA cycle is of vital importance for a large number of biosynthetic processes and plays an important role in the carbon metabolism of plants. Here we have evaluated a model of the TCA cycle with respect to its dynamic capabilities. Starting with the structural properties, as described by the stoichiometry and the elementary flux modes, we have aimed for the transition from structure to dynamics of the pathway. In particular, structural properties alone are not sufficient to determine the dynamics and function of cellular systems (Ingram *et al.*, 2006). Nonetheless, structural properties put constraints on the possible dynamics (Klipp *et al.*, 2004; Liebermeister & Klipp, 2005) and dynamic properties seem to contribute to the large-scale organization of biological networks (Prill *et al.*, 2005).

Within the approach described here, we make use of the fact that the local linear approximation of a metabolic system, the Jacobian matrix, is already sufficient to determine essential dynamic properties of the system. Based on a recently proposed method, our approach consists of generating large ensembles of possible models (Jacobians) that are consistent with the network structure of the pathway. It is thus possible to evaluate the dynamical capabilities of a metabolic system, without referring to any particular explicit set of differential equations.

With respect to the plant mitochondrial TCA cycle, this allows to identify ranges of steady state flux values and metabolite concentrations for which the system is maximally stable. Furthermore, given an experimentally observed steady state, we can identify specific biochemical conditions – in terms of (normalized) saturation of reactions – that ensure the stability of the observed steady state. Though not yet conclusive, a comparison with experimental results indicates that these dynamic requirements for maximal stability hold under wildtype conditions.

As our approach relies only upon a minimal amount of additional information about the system, it is readily applicable to metabolic system of a realistic complexity. In particular when no, or only little, knowledge about the detailed reaction mechanisms is available, our methods allows to give a systematic and comprehensive evaluation of the generalized parameter space. As compared to explicit kinetic modeling, based on explicit differential equations, the computational costs are low. Nonetheless, we emphasize that within the generalized parameter space the evaluation of the Jacobian with respect to possible instability is exact – there is no approximation involved. Future investigations will aim to provide a more detailed model of the mitochondrial TCA cycle, including adjacent reactions and the interaction of the cycle with other compartments.

## ACKNOWLEDGEMENTS

RS acknowledges financial support by HWP 2004-2006 of the state Brandenburg. TG and BB acknowledge support from the German VW-Stiftung and SFB 555.

## APPENDIX

### Structural Kinetic Modeling

Our approach is based upon a generalized parameterization of metabolic networks and a subsequent decomposition of the Jacobian into a product of two matrices (Steuer *et al.*, 2006). The time evolution of a metabolic system, consisting of $m$ metabolites $\mathbf{S} = [S_1, \ldots, S_m]$ and $r$ reactions $\boldsymbol{\nu}(\boldsymbol{S}) = [\nu_1(\boldsymbol{S}), \ldots, \nu_r(\boldsymbol{S})]$, is given as $\dot{\mathbf{S}} = \mathbf{N}\boldsymbol{\nu}(\mathbf{S})$, where $\mathbf{N}$ denotes the stoichiometric matrix. Assuming the existence of a (not necessarily unique or stable) steady state $\mathbf{S^0}$ with a steady state flux distribution $\boldsymbol{\nu^0} = \boldsymbol{\nu}(\mathbf{S^0})$, the system of differential equations can be rewritten as

$$\frac{\mathrm{d}}{\mathrm{d}t}\frac{S_i}{S_i^0} = \sum_{k=1}^{r} \underbrace{\frac{\nu_k^0}{S_i^0} N_{ik}}_{:=\Lambda_{ik}} \underbrace{\frac{\nu_k(\mathbf{S})}{\nu_k^0}}_{:=\mu_k(\mathbf{S})} \quad . \tag{2}$$

To evaluate the dynamical capabilities of the metabolic system, we aim at a parametric representation of the Jacobian matrix. Using the normalized variables $x_i(t) = S_i(t)/S_i^0$ and the definitions given in Eq. (2), the Jacobian with respect to the new variables $\mathbf{x}$ at the steady state $\mathbf{x^0} = \mathbf{1}$ is

$$\mathbf{J_x} = \boldsymbol{\Lambda}\,\boldsymbol{\theta_x^\mu} \qquad \text{with} \qquad \boldsymbol{\theta_x^\mu} := \left.\frac{\partial \boldsymbol{\mu}(\mathbf{x})}{\partial \mathbf{x}}\right|_{\mathbf{x^0}=\mathbf{1}} \tag{3}$$

Within our approach, the nonzero elements of the matrices $\boldsymbol{\Lambda}$ and $\boldsymbol{\theta_x^\mu}$ define the new generalized *parameter space* of the system, i.e. we evaluate the possible dynamics of the system in terms of the new parameters $\boldsymbol{\Lambda}$ and $\boldsymbol{\theta_x^\mu}$. Importantly, the elements of both matrices have a well-defined and straightforward interpretation in biochemical terms: The elements $\Lambda_{ik}$ of the $m \times r$ dimensional matrix $\boldsymbol{\Lambda}$ are entirely specified by experimentally accessible quantities, such as average metabolite concentrations and flux values. The elements $\theta_x^\mu$ of the $r \times m$ dimensional matrix $\boldsymbol{\theta_x^\mu}$ are closely related to the elasticity coefficients of metabolic control analysis and measure the normalized degree of saturation of each reaction. For almost all biochemical rate functions, the saturation parameters $\theta_x^\mu$ are confined to well-defined intervals (Steuer *et al.*, 2006): $\theta_x^\mu \in [0, 1]$ if the metabolite $x$ is a substrate of the reaction $\mu$. The limits $\theta_x^\mu = 1$ and $\theta_x^\mu = 0$ correspond to the linear regime ($S_i^0 \to 0$) and full

saturation ($S_i^0 \to \infty$), respectively. For cooperative and sigmoidal kinetics $\theta_x^\mu \in [0, n]$, with $n$ denoting a positive integer. Allosteric activators and inhibitors are parameterized as $\theta_x^\mu \in [0, n]$ and $\theta_x^\mu \in [0, -n]$, respectively. For mathematical details and examples see also (Steuer *et al.*, 2006).

### A Simple Example

To briefly illustrate the generalized parameterization more clearly, we consider the simplest possible metabolic pathway, consisting of $r = 2$ reactions and $m = 1$ metabolite,

$$\xrightarrow{\nu_1} S \xrightarrow{\nu_2(S)}$$

with the stoichiometric matrix $\mathbf{N} = \begin{bmatrix} 1 & -1 \end{bmatrix}$ and the (as yet unspecified) vector of rate equations

$$\boldsymbol{\nu}(\mathbf{S}) = \begin{bmatrix} \nu_1 \\ \nu_2(S) \end{bmatrix} .$$

Within our approach, the pathway is described in terms of an average metabolite concentration $S^0$, a steady state flux value $\nu^0$ and the (normalized) saturation $\theta_S^{\nu_2} \in [0, 1]$ of reaction $\nu_2$ with respect to its substrate $S$. Thus, according to Eq. (2), the generalized parameter matrices are

$$\boldsymbol{\Lambda} = \begin{bmatrix} \frac{\nu^0}{S^0} & -\frac{\nu^0}{S^0} \end{bmatrix} \qquad \boldsymbol{\theta_x^\mu} = \begin{bmatrix} 0 \\ \theta_S^{\nu_2} \end{bmatrix} . \tag{4}$$

This parameterization has several advantages compared to the more usual description in terms of Michaelis constants and maximal reaction velocities: *i)* The parameters are intuitively accessible: Even without detailed knowledge of the kinetic mechanisms it is usually possible to define a physiologically plausible range for each parameter, i.e. to specify intervals $S^0 \in [S^{\min}, S^{\max}]$, $\nu^0 \in [\nu^{\min}, \nu^{\max}]$, and $\theta_S^{\nu_2} \in [0, 1]$ that define the physiologically admissible *parameter space* of the system. *ii)* The parameterization is independent of the specific choice of the explicit functional form of the rate equations. All results obtained in terms of the generalized parameters hold for a large class of possible biochemical rate functions (Steuer *et al.*, 2006). *iii)* The generalized parameters define the corresponding Jacobian matrix at each point in parameter space. Thus, according to Eq. (3),

$$\mathbf{J_x} = \boldsymbol{\Lambda}\, \boldsymbol{\theta_x^\mu} = -\frac{\nu^0}{S^0}\theta_S^{\nu_2} \tag{5}$$

Note that Eq. (3) holds for metabolic pathways of arbitrary size and complexity.

Once the parametric representation of the Jacobian is obtained, the possible dynamics of the system can be evaluated. In particular, the eigenvalues of the Jacobian matrix define the response of the system to (small) perturbations, possible transitions to instability and the existence of oscillatory regions within the parameter space. Moreover, by taking bifurcations of higher codimension into account, the existence of complex dynamics can be predicted (Steuer *et al.*, 2006).

### An Explicit Model of the TCA cycle

The numerical simulation shown in Fig. 7 is based on an explicit model of the cycle. All reactions, except $\nu_5$ and $\nu_6$, were modeled as mass-action kinetics with $\nu_i = k_i \prod S_j$. Given a desired steady state from the random ensemble, the kinetic parameters are $k_i = \nu_i^0 / \prod S_j^0$. Product inhibition of Pyr and OAA on their production was incorporated as $\nu_5 = k_5[\mathrm{Mal}]/(1 + \frac{[\mathrm{OAA}]}{K_{\mathrm{m5}}})$ and $\nu_6 = k_6[\mathrm{Mal}]/(1 + \frac{[\mathrm{Pyr}]}{K_{\mathrm{m6}}})$, respectively. The parameters $K_{\mathrm{m5}}$ is determined as a function of the saturation parameter $\theta^5_{\mathrm{OAA}} = 0.1$, $K_{\mathrm{m5}} = [\mathrm{OAA}]^0(1 - \theta^5_{\mathrm{OAA}})/\theta^5_{\mathrm{OAA}}$. Analogously for $K_{\mathrm{m6}}$. Note that the existence of the Hopf bifurcation does not depend on the particular explicit form of the rate equation.

### Evaluation of the Structural Kinetic Model

To evaluate the properties of the TCA cycle at a particular steady state (Fig. 8), the (relative) flux distribution was chosen according to (Hanning & Heldt, 1993; Schwender *et al.*, 2004). Metabolite concentration were based upon the measurements given in (MacDougall & ap Rees, 1991; Farré *et al.*, 2001). In case no mitochondrial concentration was available, the respective concentration was replaced by its value in the cytosol.

## REFERENCES


Famili, I., Förster, J., Nielsen, J. & Palsson, B. O. (2003). *Saccharomyces cerevisiae* phenotypes can be predicted by using constraint-based analysis of a genome-scale reconstructed metabolic network. *Proc. Nat. Acad. Sci.*, **100**, 13134–13139.

Farré, E. M., Tiessen, A., Roessner, U., Geigenberger, P., Trethewey, R. N. & Willmitzer, L. (2001). Analysis of the compartmentation of glycolytic intermediates, nucleotides, sugars, organic acids, amino acids, and sugar alcohols in potato tubers using a nonaqueous fractionation method. *Plant Physiol.*, **127**, 685–700.

Fernie, A. R., Trethewey, R. N., Krotzky, A. J. & Willmitzer, L. (2004). Metabolite profiling: from diagnostics to systems biology. *Nature Reviews, Molecular Cell Biology*, **5**, 1–7.

Hanning, I. & Heldt, H. W. (1993). On the function of mitochondrial metabolism during photosynthesis in spinach leaves. *Plant Physiol.*, **103**, 1147–1154.

Heinrich, R. & Schuster, S. (1996). The Regulation of Cellular Systems. Chapman & Hall, New York.

Hill, S. A. (1997). Carbon metabolism in mitochondria. In Dennis, D. T., Turpin, D. H., Lefebvre, D. D. & Layzell, D. B., (eds.) *Plant Metabolism*. Addison Wesley Longman, Harlow, UK, second edition, pp. 181–199.

Ingram, P. J., Stumpf, M. P. H. & Stark, J. (2006). Network motifs: structure does not determine function. *BMC Genomics*, **7**, 108.

Klipp, E., Liebermeister, W. & Wierling, C. (2004). Inferring dynamic properties of biochemical reaction networks from structural knowledge. *Genome Informatics Series*, **15**, 125–137.

Liebermeister, W. & Klipp, E. (2005). Biochemical networks with uncertain parameters. *IEE Proc. Systems Biology*, **152**, 97–107.

MacDougall, A. J. & ap Rees, T. (1991). Control of the Krebs cycle in *arum* Spadix. *J. Plant Physiol.*, **137**, 683–690.

Prill, R. J., Iglesias, P. A. & Levchenko, A. (2005). Dynamic properties of network motifs contribute to biological network organization. *PLoS Biol.*, **3**, 1881–1892.

Ronen, M., Rosenberg, R., Shraiman, B. I. & Alon, U. (2002). Assigning numbers to the arrows: Parameterizing a gene regulation network by using accurate expression kinetics. *PNAS*, **99**, 10555–10560.

Schuster, S., Dandekar, T. & Fell, D. A. (1999). Detection of elementary flux modes in biochemical networks: a promising tool for pathway analysis and metabolic engineering. *TIBTECH*, **17**, 53–60.

Schuster, S., Fell, D. A. & Dandekar, T. (2000). A general definition of metabolic pathways useful for systematic organization and analysis of complex metabolic systems. *Nat. Biotechnol.*, **18**, 326–332.

Schwender, J., Ohlrogge, J. & Shacher-Hill, Y. (2004). Understanding flux in plant metabolic networks. *Curr. Opinion in Plant Biology*, **7**, 309–317.

Stelling, J., Klamt, S., Bettenbrock, K., Schuster, S. & Gilles, E. D. (2002). Metabolic network structure determines key aspects of functionality and regulation. *Nature*, **420**, 190–193.

Steuer, R., Gross, T., Selbig, J. & Blasius, B. (2006). Structural kinetic modeling of metabolic networks. *Proc. Natl. Acad. Sci. USA*, **103**, 11868–11873.

Sweetlove, L. J. & Fernie, A. R. (2005). Regulation of metabolic networks: Understanding metabolic complexity in the systems biology era. *New Phytologist*, **168**, 9–24.